

empty empty itletempty

ABSTRACT

In this work we studied the regional manifestations of space weather at central Mexico through isolate the local geomagnetic response from its planetary counterpart. In order to do so, we analyzed 20 intense geomagnetic storms by identifying the ionospheric contribution in their regional geomagnetic data as registered at the Magnetic Observatory of Teoloyucan (at the north of Mexico City). Our analysis indicated that local geomagnetic response is mainly driven by ionospheric disturbances. We also found that the *disturbed polar current number 2* and the *disturbed dynamo current* are particularly relevant for the regional geomagnetic response. Additionally, we showed that regional geomagnetic activity can be approximated by the combined effects of the planetary geomagnetic response and the regional magnetic perturbations induced by the commented ionospheric currents. Finally, our results highlights the particularities that geomagnetic response has in different locations.

Highlights

Low latitude geomagnetic response associated with intense geomagnetic storms: regional space weather in Mexico

Castellanos-Velazco, C. I., Corona-Romero, P., González-Esparza, J. A., Caccavari-Garza, A. L., Sergeeva, M. A., Gatica-Acevedo, V. J.

- Research of space weather activity over center of Mexico
- Analysis of differences in local and planetary geomagnetic responses during a geomagnetic storm.
- Study of ionospheric currents related to geomagnetic storms, known to drive local geomagnetic fluctuations.

 ccastellanos@igefisica.unam.mx (C.C. I.);
p.coronaromero@igefisica.unam.mx (C. P.); amarico@igefisica.unam.mx
(G.J. A.)
ORCID(s): 0000-0001-8818-5318 (C.C. I.); 0000-0002-2573-2967 (C. P.);
0000-0003-4774-1829 (G.J. A.)

Low latitude geomagnetic response associated with intense geomagnetic storms: regional space weather in Mexico

Castellanos-Velazco, C. I.^a, Corona-Romero, P.^{b,c}, González-Esparza, J. A.^c, Caccavari-Garza, A. L.^d, Sergeeva, M. A.^{b,c} and Gatica-Acevedo, V. J.^{c,**}

^aPosgrado en Ciencias de la Tierra, Universidad Nacional Autónoma de México, Cto. de los Posgrados S/N, C.U., Ciudad de México, 04510, Ciudad de México, México.

^bInvestigadores por México-CONAHCYT (CONAHCYT Research Fellow), Instituto de Geofísica Unidad Michoacán, Universidad Nacional Autónoma de México, Morelia, Michoacán, México.

^cLaboratorio Nacional de Clima Espacial (LANCE), Instituto de Geofísica Unidad Michoacán, Universidad Nacional Autónoma de México, Antigua Carretera a Pátzcuaro 8701, Morelia, 58089, Michoacán, México.

^dInstituto de Geofísica, Universidad Nacional Autónoma de México, Av. Universidad 3000, México city, 04150, México.

ARTICLE INFO

Keywords:

Space Weather
Geomagnetic Storms
Regional Response
Ionospheric Currents
Disturbed Dynamo
Disturbed Polar Current 2

ABSTRACT

In this work we studied the regional manifestations of space weather at central Mexico through isolate the local geomagnetic response from its planetary counterpart. In order to do so, we analyzed 20 intense geomagnetic storms by identifying the ionospheric contribution in their regional geomagnetic data as registered at the Magnetic Observatory of Teoloyucan (at the north of Mexico City). Our analysis indicated that local geomagnetic response is mainly driven by ionospheric disturbances. We also found that the *disturbed polar current number 2* and the *disturbed dynamo current* are particularly relevant for the regional geomagnetic response. Additionally, we showed that regional geomagnetic activity can be approximated by the combined effects of the planetary geomagnetic response and the regional magnetic perturbations induced by the commented ionospheric currents. Finally, our results highlights the particularities that geomagnetic response has in different locations.

1. Introduction

Geomagnetic storms (GS) are significant phenomena within space weather, as they can adversely impact various systems such as communications, navigation, and energy supply (Schrijver, 2015). GSs are closely tied to solar activity and primarily involve a temporary weakening of the Earth's magnetic field (EMF), among other effects (Gonzalez et al., 1994). These storms arise when solar wind material penetrates the EMF through magnetic reconnection between the interplanetary magnetic field (IMF) and the EMF Baumjohann and Treumann (1999); C.T Russell (2016).

Geomagnetic storms are typically identified using geomagnetic indices, which quantify their magnitude. Various geomagnetic indices exist, each designed to capture specific aspects of geomagnetic disturbances. In the context of middle and low latitudes, the most commonly used indices are the planetary K index (K_p) and the disturbance storm time index (Dst). These indices are especially effective in regions where the geomagnetic perturbation can be observed on the Earth's magnetic field's horizontal component (H). The K_p index quantifies the maximum variation in H observed at mid-latitudes over three-hour intervals. Similarly, the Dst index represents an hourly average of perturbations in H as measured near the Earth's magnetic equator. These planetary

indices, namely K_p and Dst, have regional counterparts that rely on regional data instead of planetary averages (Mayaud, 1980).

While geomagnetic storms are global phenomena, their manifestation at the regional scale can exhibit variability across different locations. This variation can be attributed to the Earth's heterogeneity, asymmetries in magnetospheric and ionospheric currents, and the intricate interactions between the magnetosphere and ionosphere in each region. Consequently, geomagnetic latitude, local time, and seasonal variations can influence how a geomagnetic storm unfolds at the regional level. Overlooking these regional factors may lead to uncertainties and misinterpretations when attempting to comprehend and address the potential effects of geomagnetic storm events (Pirjola, 2000; Bailey et al., 2017; Vodyannikov et al., 2006; da Silva Barbosa et al., 2015).

In recent decades, there has been growing interest in regional space weather. Regional space weather studies mainly focuses on identified the differences between the local and planetary geomagnetic and ionospheric responses. Because such differences, combined with the regional distribution of infrastructure, facilities and services demand might help to management risks due to space weather (see Hejda and Bochníček, 2005; da Silva Barbosa et al., 2015; Bailey et al., 2017, and references there in). Recently, Mexico has joint this regional space weather sudties by conduct scattered regional ionospheric and geomagnetic studies (Pérez-Enríquez and Kotsarenko, 2003; Gonzalez-Esparza

*Corresponding author

 ccastellanos@igeofisica.unam.mx (C.C. I.)

p.coronaromero@igeofisica.unam.mx (C. P.); americoo@igeofisica.unam.mx (G.J. A.)

ORCID(s): 0000-0001-8818-5318 (C.C. I.); 0000-0002-2573-2967 (C. P.); 0000-0003-4774-1829 (G.J. A.)

et al., 2005; Rodriguez-Martinez et al., 2011; Carrillo-Vargas et al., 2012; Rodriguez-Martinez et al., 2011; López-Montes et al., 2012; Rodriguez-Martinez et al., 2014; Merlin Matamba et al., 2016; Martínez-Bretón L. et al., 2016). However, the systematic study and monitoring of regional space weather formally commenced in 2014 with the initiation of operations by the Mexican Space Weather Service (SCIESMEX) at the Geophysics Institute (IGF) of the National Autonomous University of Mexico (UNAM). Subsequently, by 2016, a significant expansion of infrastructure and technologies dedicated to studying and monitoring regional space weather was achieved by establishing the Mexican Space Weather National Laboratory (LANCE) at IGF-UNAM (Gonzalez-Esparza et al., 2017).

Through collaborative efforts and resource sharing, the SCIESMEX/LANCE collaboration has identified the potential role of ionospheric disturbances in driving regional geomagnetic response during geomagnetic storm periods (see Romero-Hernandez et al., 2017; Sergeeva et al., 2017, 2019; Corona-Romero et al., 2018, 2017). This finding aligns with other studies conducted in mid and low latitudes, as it is known that for these latitudinal ranges, two primary sources of geomagnetic fluctuations driven by ionospheric currents exist: the *disturbed polar current number 2* (DP2) (Nishida, 1968a,b, 1966), and the *disturbed dynamo current* (Ddyn) (Blanc and Richmond, 1980).

On one hand, the DP2 current is linked to electric fields induced during the magnetic reconnection between the interplanetary magnetic field and the EMF. These electric fields are then transported along the Birkeland currents (Wei et al., 2015; Kikuchi and Hashimoto, 2016), eventually reaching high ionospheric latitudes where they give rise to a pattern of two ionospheric convective twin cells known as DP2 currents. The charged particles within these cells are carried by the centrifugal and curvature effects of the EMF, resulting in the induction of a polarized electric field (Heppner, 1972b,a; Bobova et al., 1985; Blanc and Caudal, 1985; Denisenko et al., 1992). During the main phase of a geomagnetic storm, this polarized electric field, coupled with the DP2 current, can extend beyond high latitudes, encompassing mid and even low latitudes (Nishida, 1966, 1968a; Obayashi and Nishida, 1968).

On the other hand, Ddyn currents represent amplifications of the polar ionospheric currents due to the precipitation of energetic particles during the main phase of a geomagnetic storm. The resulting Joule heating in the thermosphere generates the circulation of neutral winds and charged particles in the equatorward direction. The Coriolis force induces a westward shift in the direction of these polar-equatorial flows at mid and low latitudes (Blanc and Richmond, 1980; Le Huy and Amory-Mazaudier, 2005; Zaka et al., 2009). Equatorward Pedersen currents are induced in this process, leading to the accumulation of charged particles along the dip equator. This accumulation, in turn, triggers the generation of poleward-directed electric fields and a second Pedersen current in the same direction but opposing the first one. Consequently, Hall currents are driven eastward

at mid-latitudes (approximately 45°), and these currents are interrupted at termination points (Blanc and Richmond, 1980). This sequence of events results in currents diverging and closing at adjacent latitudes, forming the distinct vortex-shaped currents known as Ddyn.

Previous studies indicate that the effects associated with Ddyn and DP2 locally disrupt the total electron content, causing significant impacts on services such as telecommunications and global positioning systems during periods of geomagnetic storms (GMTs), regardless of geomagnetic latitude (?). In the case of Mexico, a local ionospheric response has been observed even when the Dst index is only slightly perturbed (Sergeeva et al., 2017, 2019). Given that the Ddyn and DP2 ionospheric currents possess the potential to influence the geomagnetic response in mid and low latitudes, it raises the question of whether these ionospheric mechanisms are responsible for linking regional geomagnetic response to local ionospheric perturbations in central Mexico. This inquiry constitutes the primary motivation for our study.

Throughout this work, we first seek to identify disparities between regional and planetary geomagnetic activities to isolate regional geomagnetic responses during geomagnetic storms. With this regional response isolated, we search for evidence of Ddyn and DP2 mechanisms as sources of such regional geomagnetic response. Our approach involves identifying their respective signatures within magnetic records. Subsequently, we validate our findings by comparing planetary and regional geomagnetic activity indices, culminating in a discussion of our concluding remarks. In the next section, we present the methodology employed to accomplish these objectives and provide further insights into the specifics of our investigation.

2. Methodology

2.1. Local geomagnetic response

We analyzed 20 geomagnetic storm (GS) events to identify the regional geomagnetic response. These events occurred during the period from 2003 to 2018, encompassing the descending phase of solar cycle 23 and almost all of solar cycle 24. The data were recorded at the Geomagnetic Observatory of Teoloyucan (TEO), located at 27.84°N and 28.41°W. TEO is operated by the Magnetic Service of the Geophysics Institute at the National Autonomous University of Mexico. We selected events with a local K index (K_{TEO}) equal to or larger than 6+ and ΔH_{TEO} (the regional equivalent of the Dst index) below -120 nT. We also rejected events whose datasets contained a considerable amount of missing data. Table 1 provides details of all the analyzed events.

We assume that significant differences between regional and planetary geomagnetic indices should be provoked by local geomagnetic response. Thus, in order to identify such differences we directly compare Dst and ΔH_{TEO} for our studied events. Figure 1 shows a dispersion plot that compares the regional response (vertical axis) with its planetary counterpart (horizontal axis). In the figure we observe two well differentiated tendencies in data distribution: The first

Table 1

Study Cases: Event Number, Start Date of GS Main Phase, Minimum (Maximum) Values Reached during the Events for Dst (K_p) and ΔH_{TEO} (K_{TEO}) Geomagnetic Indices, Respectively.

Event #	Beginning of main phase	^a Dst minimum [nT]	^b ΔH minimum [nT]	^a K_p maximum	^b K_{TEO} maximum
1	2003/05/29	-144	-190	8+	9
2	2003/10/14	-85	-126	7+	7-
3	2003/11/20	-422	-441	9-	9
4	2004/07/22	-170	-167	9-	8+
5	2004/08/30	-129	-154	7	7-
6	2004/11/08	-374	-398	9-	9
7	2005/05/15	-247	-206	8+	7
8	2005/06/12	-106	-120	7+	6+
9	2005/08/24	-184	-138	9-	9-
10	2005/08/31	-122	-125	7	6+
11	2006/08/19	-79	-131	6	7-
12	2006/12/14	-162	-247	8+	9
13	2015/03/15	-222	-282	8	8-
14	2015/10/07	-124	-143	7+	7+
15	2015/12/20	-155	-189	7-	7
16	2016/03/06	-98	-120	6	7
17	2016/10/13	-104	-128	6+	6+
18	2017/05/27	-125	145	7	8
19	2017/09/07	-124	-170	8+	8+
20	2018/09/25	-175	-176	7+	7-

Comments for the Table.

^a Dst and Kp were obtained from the International Service of geomagnetic Indices (ISGI).

^b Regional geomagnetic indices ΔH_{TEO} and K_{TEO} were computed by the Space Weather National Laboratory, using TEO geomagnetic registers.

one ($Dst \geq -100$ nT) where the data points closely follow the identity (solid black line), and the second one (green shadowed region) where the data dispersion detached from the identity ($Dst < -100$ nT). This appreciation is agreement with the correlation indices of each region, which gives $R^2 = 0.77$ for the first one, and $R^2 = 0.42$ for the latter.

Figure 1 shows, in the case of our analyzed events, that planetary and regional geomagnetic indices may significantly differ each other. Which in turn suggests the presence of some kind of local (ionospheric) mechanisms with the capability to deviate the regional value of geomagnetic field from its planetary counterpart. Hence, we need to identify in the regional geomagnetic registers the signatures for the magnetic contribution cause by those ionospheric mechanisms (Le Huy and Amory-Mazaudier, 2005; Zaka et al., 2009; Amory-Mazaudier et al., 2017; Younas et al., 2020). Now we proceed to identify such mechanisms.

2.2. Geomagnetic signatures of local ionospheric currents

The local values of EMF are result from the contribution of many sources (Rishbeth and Garriott, 1969; Knecht and B.M, 1985; Gjerloev, 2012; van de Kamp, 2013). In the particular case of the horizontal component (H) of local EMF, we can express it as:

$$H = B_{SQ} + H_0 + D_M + D_I, \quad (1)$$

where B_{SQ} is the diurnal variation obtained from the local quiet days (van de Kamp, 2013); H_0 is the day-to-day variation (Gjerloev, 2012; van de Kamp, 2013). The last two terms are irregular magnetic variations related to geomagnetic activity (Le Huy and Amory-Mazaudier, 2005; Zaka et al., 2009): with D_M being the contribution from (planetary scale) magnetospheric currents, and D_I is the magnetic contribution driven by ionospheric perturbations. Furthermore, in the case of mid and low latitudes, $Dst \cdot \cos(\lambda)$ can be approximation D_M with λ being the geomagnetic latitude (Amory-Mazaudier et al., 2017). such approximation transforms Equation 1 into:

$$D_I \approx H - (B_{SQ} + H_0 + Dst \cdot \cos(\lambda)). \quad (2)$$

In addition, D_I can be expressed as:

$$D_I = DP2 + D_{dyn} + D_{others}, \quad (3)$$

with D_{others} , we refer to ionospheric perturbations distinct from the disturbed polar current number 2 ($DP2$) and the disturbed dynamo current (D_{dyn}). These two ionospheric

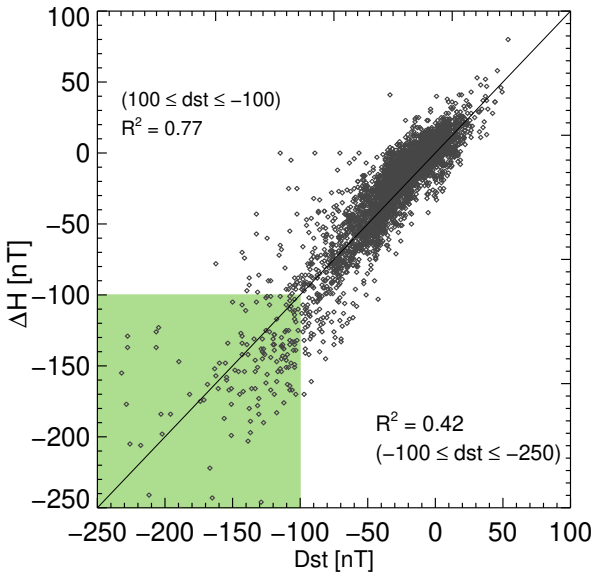


Figure 1: Dispersion plot illustrating ΔH (vertical axis) in relation to Dst (horizontal axis) for all Geomagnetic Storm (GS) events. The green region highlights a -100 nT threshold, where a secondary R^2 calculation was performed.

currents are well accepted sources for local geomagnetic fluctuations in low and mid geomagnetic latitudes, as discussed in the Introduction.

3. Analysis and results

3.1. Local ionospheric disturbances and induced magnetic fluctuations

In this section, we present our analysis process through analyzing event 13. The panel (a) of Figure 2 shows the profiles of Dst (black) and ΔH (green) indices during the GS associated with event 13 (see Table 1). In the panel, we observe that both indices are *quiet* up to the start of the GS's main phase, signed out by a vertical dotted line. The main phase lasts approximately one day, reaching a minimum of $Dst \sim -300$ nT, whereas the recovering phase extends almost three days.

In the panels (b) of Figure 2, we appreciate the resulting profile of D_I (Equation (2)), which we computed using the TEO's registers and the Dst reported data. Subsequently, we construct a power spectrum for our computed profile of D_I , which we show in panels (d) of Figures 2. In the power spectrum, we highlight, by a gray shading, the range of periods(frequencies) consistent with $DP2$ and $Ddyn$. In the panel, we identify $Ddyn$'s range by setting the main period and searching potency peaks within the range of possible harmonics. It is important to remark that, because our study cases might be potentially different from each other, the filtering ranges might vary slightly from case to case.

In panels (c) of Figure 2 we present the profiles of the induced magnetic perturbations caused by $DP2$ (solid red line) and $Ddyn$ (solid black line). These profiles are constructed

departing from the frequencies identified through the filtering process commented on in the previous paragraph. We note that the enhancements of the induced effects of $Ddyn$ and $DP2$ simultaneously occur with an increase in the total electron content over central Mexico, as the panels (e) of Figure 2 shows.

We applied the procedure presented in this section to all our study cases. The Figures 6 and 7 in the Appendix show the computed D_I and the resulting profiles of $DP2$ and $Ddyn$, for each event in Table 1. We remark on the uniqueness of each event, which is clear in the D_I profiles and its associated magnetic perturbations induced by $DP2$ and $Ddyn$ currents.

In general, we noted that the amplitude of the magnetic oscillations induced by $Ddyn$ are more intense than those induced by $DP2$ (see Figures 6 and 7 at the Appendix). This suggests that, in most cases, $Ddyn$'s induced magnetic effects are dominant on the local EMF. Although there are events for which both effects show similar intensities. We think of two possibilities to explain that: The first is the process that triggers the GS itself, *i.t.* the solar activity event, and its magnetic reconnection with the EMF. This may affect the evolution of the ionospheric response, directly modifying the evolution of $DP2$ and $Ddyn$ currents. Secondly, we have to consider that our data is sampled in hourly resolution. In this case, data sampling represents an important limitation since $DP2$ magnetic fluctuations, as mentioned in Nishida (1968b), may have periods of less than an hour or even of tens of minutes. In this scenario, we possibly missed part of $DP2$ fluctuations during our analysis. This could be solved, in principle, by using $Sym - H$ index rather than Dst , a task in which exploration we consider our future work.

3.2. Validation of $DP2$ and $Ddyn$ magnetic signatures

In Section 2.1 we were able to identify significant differences between the planetary and regional geomagnetic activity. Condition that we associated to regional geomagnetic response. Subsequently, in Section 3.1, we identified the tentative geomagnetic mechanisms for that regional geomagnetic response. Such mechanism are the $Ddyn$ and $DP2$ ionospheric currents, whose effects were reconstructed by a periods (frequencies) filtering process. We also learned that those effects are systematically associated with local perturbations on TEC. Now, we require to validate our results.

In order to validate our previous results, first we approximate the regional geomagnetic index ΔH , which can be defined as:

$$\Delta H = H - (B_{SQ} + H_0), \quad (4)$$

through Dst and the resulting profiles of $DP2$ and $Ddyn$. Thus, by manipulating Equations (2), (3) and (4) we obtain that:

$$\Delta H \approx Dst \cos(\lambda) + DP2 + Ddyn. \quad (5)$$

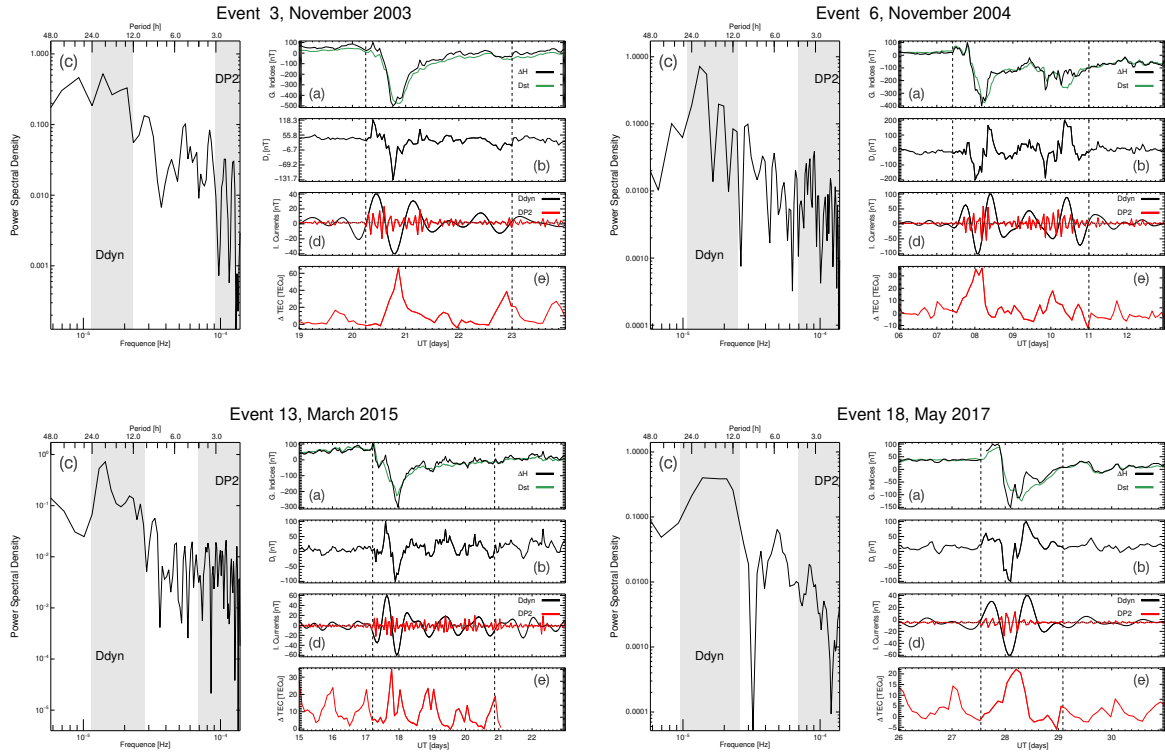


Figure 2: Analysis examples from solar cycle 23 (upper panels) and solar cycle 24 (bottom panels). Upper(bottom) panels show the analysis of events 3(13) and 6(18). The analysis of each event is made up of five different processes represented by panels labeled with letters. Panels (a) present the values of Dst (black line) and ΔH (green line) indices during the event. Panels (b) show the computed value of D_I . Panels (c) show the power spectrum associated to D_I . Panels (d) show the induced geomagnetic effects of $Ddyn$ (in black) and $DP2$ (in red) reconstructed from the filtered power spectrum. Panels (e) show the variation of the total electron content (ΔTEC) over the central region of Mexico. The dotted vertical lines in panels (a), (b), (d) and (e) mark out the start (left-sided) and end (right-sided) of the Geomagnetic Storm (GS). Gray shaded regions in panel (c) highlight the bandwidths associated with $Ddyn$ and $DP2$ filters.

For simplicity, we call Dst_λ the combined effects of $Dst \cos(\lambda)$, $DP2$ and $Ddyn$. Hence, our first step for validation is to corroborate that our computed value of Dst_λ approximates ΔH . In addition, we can also used Dst_λ and the values of K_p to approximate the local value of K .

The results of the validation process commented on before applied on events 3, 13 and & 18 are shown by Figure 3. The upper panels of Figure 3 compares the profiles of ΔH (black), Dst (green) and Dst_λ (red). In the panel we note that Dst_λ is systematically closer to 2024JASTP.256062040 ΔH than Dst . This condition holds during the main and recovering phases of the GS. Additionally, in the bottom panel of Figure 3 it is clear that the planetary (green) and local (black) values of K index differ each other.

This process was repeated with all our study cases. The Figures 8 and 9 show the results of our validation exercise. In all the cases, we found that Dst_λ consistently approximates ΔH . We also found that K_p with the combined effects of Dst_λ was able to enclose the regional K values.

Now, in addition to our previous qualitative comparison; we proceed with a quantitative exploration. For this purpose we compute the average absolute difference between

the pairs $\Delta H - Dst$ and $\Delta H - Dst_\lambda$ for our study cases. The results for this exploration are shown by Figure 4. In the figure we observe a histogram with the average difference between $\Delta H - Dst$ (blue bars) and $\Delta H - Dst_\lambda$ (red bars). We note that average difference associated with Dst_λ is systematically lesser than that associated with Dst . This result indicates that the effects of magnetic perturbations consistent with those provoked by $DP2$ and $Ddyn$ are relevant for regional geomagnetic response.

Finally, our third and last step for our validation process is to remake the dispersion plot of Figure 1, but using Dst_λ data instead of Dst 's. Figure 5 shows the new dispersion plot where we can appreciate, in contrast with Figure 1, that data points (open diamonds) closely follow the identity (solid black line). Furthermore, when we compute the correlation indices we obtain note that R^2 grew from 0.77 up to 0.86 for the range of $Dst \geq -100$ nT. In addition, for the case of $Dst < -100$ nT, $R^2 = 0.75$ which is significant increment from the value originally associated to Dst ($R^2 = 0.42$).

Our validation process proved that the magnetic perturbations tentatively induced by $DP2$ and $Ddyn$ ionospheric currents, when combined with planetary indices, allowed

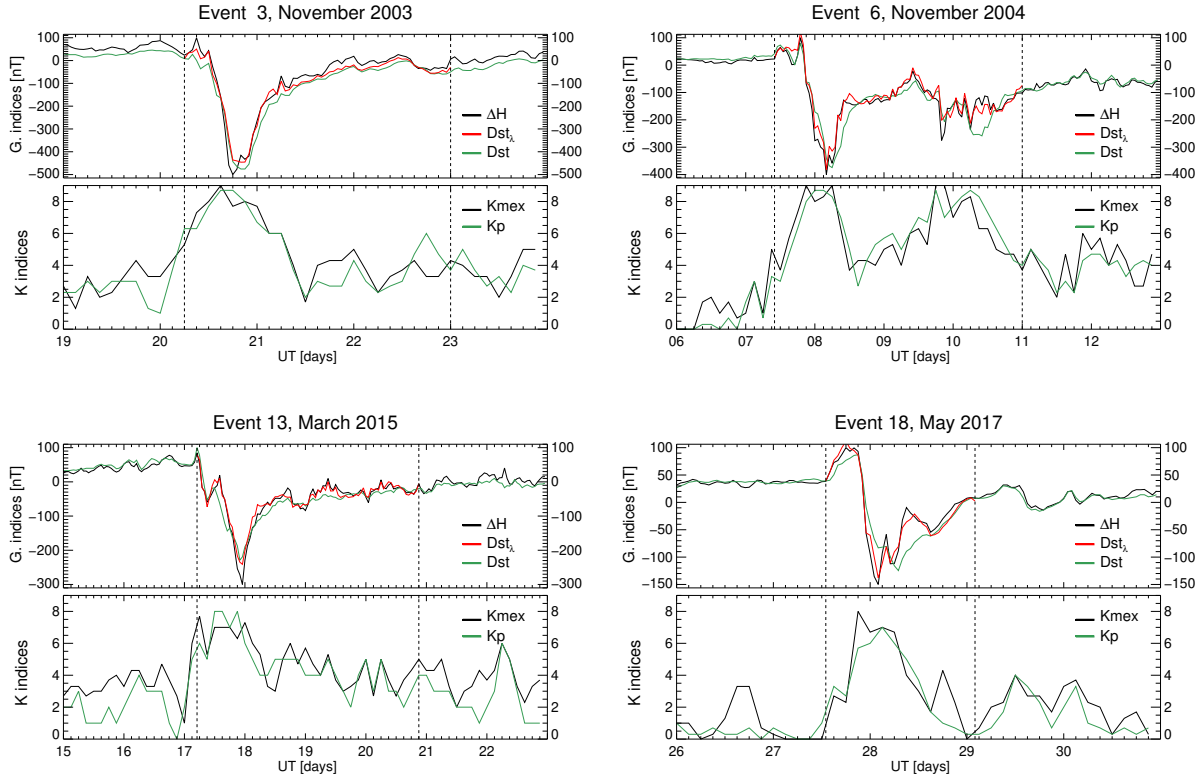


Figure 3: Comparisson between regional and planetary geomagnetic response for events 3, 6, 13 and 18. Each event shows data from Dst , ΔH , Dst_λ , K_p and K_{mex} indices. Planetary indices are depicted by green solid lines, while local geomagnetic indices are represented by black solid lines. The ΔH index is indicated by the red line

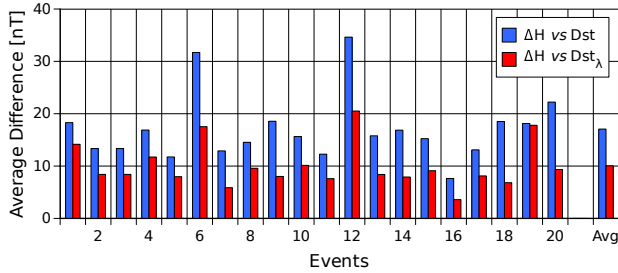


Figure 4: The average differnce between the planetary and regional geomagnetic response as registerd by Dst and ΔH indices for all the analyzed events. Blue bars represent the difference between ΔH and Dst , whereas red bars represent the difference between ΔH and Dst_λ (red bars).

to qualitatively approximate the regional geomagnetic activity. We also proved that regional geomagnetic response, as registered by ΔH , can be quantitatively expressed by the planetary response (Dst) combined with the geomagnetic effects of the already commented ionospheric currents. Finally, when including the magnetic effects induced by $DP2$ and $Ddyn$ into the planetary response, the dispersion between regional and planetary data substantially decreased.

4. Concluding remarks

In this work we studied the regional manifestations of space weather. We focused on the differences between planetary and local geomagnetic responses during periods of strong geomagnetic storms (GS) at center of Mexico. We also investigated the possible sources for such differences in the geomagnetic response. In order to do so, we used the geomagnetic registers from the Teoloyucan Magnetic Observatory (TEO), located at north of Mexico City. We also use data sets from the Dst and K_p planetary indices, as well as the regional geomagnetic index ΔH and the total electron content delivered by the Mexican Space Weather National Laboratory.

We selected 20 GS as study cases for this work (see Table 1). For all our study cases we identified evidence for the presence of relevant regional geomagnetic response through a dispersion plot (see Figure 1). In this regard, we found that in the range of $Dst < -100$ nT there is a tendency for the regional geomagnetic index to deviate from the planetary one. We assumed this as an evidence for regional geomagnetic response.

Subsequently, we isolated the geomagnetic effects due to ionospheric processes (D_I) from the regional (TEO) geomagnetic registers. Next, we applied filters on D_I with the purpose of identify the magnetic perturbations consistent with those induce by $Ddyn$ and $DP2$ currents. We also

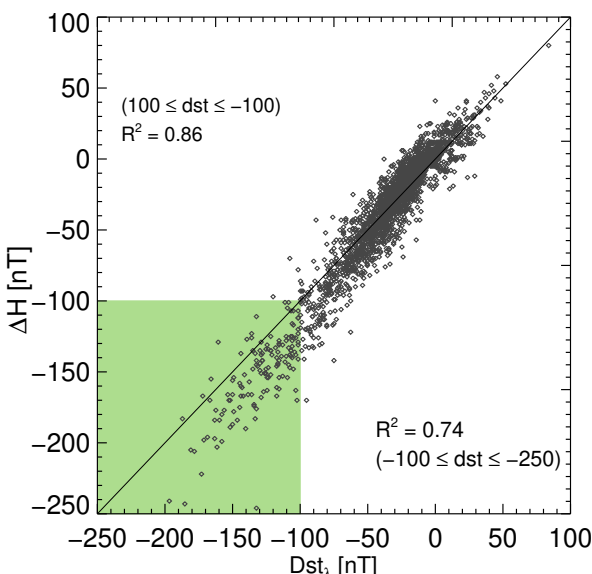


Figure 5: scatter plot illustrating ΔH (vertical axis) in relation to Dst_λ (horizontal axis) for all GS events. Within the green region, characterized by a -100 nT threshold, a secondary R^2 calculation was performed.

verified that intensification of the resulting $Ddyn$ and $DP2$ profiles simultaneously occurred during TEC perturbations (see discussion of Figure 2). In consequence, we were able to reconstruct the regional geomagnetic response consistent with those induced by $Ddyn$ and $DP2$ currents.

Afterwards, we validate our computed geomagnetic contribution due to $Ddyn$ and $DP2$ currents. First, we approximate the regional K and ΔH indices by combining the planetary K_p and Dst indices with the regional geomagnetic effects of $Ddyn$ and $DP2$. Secondly, we computed the differences between ΔH and Dst with and without the regional ionospheric effects. Finally, we analyzed the dispersion between ΔH and Dst combined with the effects of $Ddyn$ and $DP2$. For all the cases, we found that regional geomagnetic response is qualitatively and quantitatively approximated by the geomagnetic planetary response combined with the geomagnetic perturbations induced by the $Ddyn$ and $DP2$ ionospheric currents.

In this work we focus on regional space weather in Central Mexico by studying local geomagnetic and ionospheric data. We identified evidence of regional geomagnetic response that is significantly different from its planetary counterpart. We investigated $Ddyn$ and $DP2$ ionospheric currents as possible mechanisms for such a regional response. As a result, we were able to isolate the magnetic perturbations associated with those ionospheric currents, which is consistent with the local ionospheric TEC response. The combination of these perturbations with planetary response succeeded in approximate the regional geomagnetic response, i.e. the regional geomagnetic response has a significant component from local ionospheric effects.

Thus, our study shows that regional space-weather manifestations at central Mexico may significantly deviate from the planetary response. In consequence, in order to address the regional effects of, and risks due to, space-weather in Central Mexico, it is necessary to carry out studies from a regional approach, complemented with the planetary context. Our results highlight the particularities that geomagnetic response has for a given location. Hence, in order to achieve a better understanding of space weather and to improve the operational response, our results evidence for the necessity to include more registers (magnetometers) into the computing of geomagnetic indices, whether planetary or regional.

Hence, according to our results, during intense geomagnetic storms, in central Mexico, the effects of $Ddyn$ and $DP2$ may induce alterations in the F region of the ionosphere and displace the equatorial ionospheric anomaly towards central and southern regions of Mexico (as showed by ?). Therefore we could expect these phenomena lead to ionospheric scintillation, which degrades satellite communications, as well as the precision of navigation and positioning systems, among other services. All these effects can potentially be addressed through local perturbations of the TEC during geomagnetic storm periods (refer to panels (e) of Figure 2).

It is important to remark that the surface of Mexico is near 2 million km². This fact made of our results valid only for the central region of Mexico (few thousands of km²), leaving the rest of its surface to address. In addition, Mexico is located at North America, and the ionospheric currents pass through and evolve along the whole American continent. Hence, on one hand, it is required more sources of geomagnetic registers in Mexico and, on the other hand, it is necessary to contextualize the geomagnetic response of Mexico with those present in Northern and Central America, and even South America. For the first case, LANCE is developing a the Network of Geomagnetic Stations Mexico (REGMEX) (see ?), to monitoring regional geomagnetic response all over Mexico. Whereas, for the case of contextualize the geomagnetic response of Mexico, this is our immediate future work.

CRediT authorship contribution statement

Castellanos-Velazco, C. I.: Methodology, Conceptualization, Data analysis, Software, Data processing, Writing - Original Draft. **Corona-Romero, P.:** Conceptualization, Methodology, Regional indices computation, Writing - Review & Editing. **González-Esparza, J. A.:** Data revision, Review & Editing. **Caccavari-Garza, A. L.:** Regional magnetic data, Review & Editing. **Sergeeva, M. A.:** Local ionospheric data, Review & Editing. **Gatica-Acevedo, V. J.:** Local ionospheric data, Ionospheric data processing.

Declaration of competing interest

The authors declare that they have no known competing financial interests or personal relationships that could have appeared to influence the work reported in this paper.

Data Availability

Data will be made available on request.

Acknowledgments

P. Corona-Romero is grateful for Investigadores por Mexico-CONAHCYT (CONAHCYT Research Fellow) project 1045 Space Weather Service, financed by “Consejo Nacional de Ciencia y Tecnología” (CONAHCYT), which partially supported this work. C.I. Castellanos-Velazco is grateful for “La Beca de Posgrado en Mexico” granted by CONAHCYT. LANCE acknowledges partial financial support from CONHACyT-AEM grant 2017-01-292684, CONAHCyT LN-315829, and PAPIIT IN116023.

This work used data from the Teoloyucan Magnetic Observatory operated by the Magnetic Service of the Geophysics Institute at National and Autonomous University of Mexico (UNAM). Total electron content (TEC) and the geomagnetic indices ΔH and K , the regional counterparts of Dst and K_p indices respectively, are produced by the Mexican Space Weather National Laboratory (LANCE), Geophysics Institute at National and Autonomous University of Mexico (UNAM).

The results presented in this paper rely on K_p and Dst geomagnetic indices calculated by the Helmholtz-Zentrum Potsdam Deutsches GeoForschungsZentrum Adolf-Schmidt-Observatorium and the World Data Center for Geomagnetism, Kyoto, respectively, from data collected at magnetic observatories. We thank the involved national institutes, the INTERMAGNET network and ISGI.

All authors have seen and approved the final version of the manuscript.

References

- Amory-Mazaudier, C., Bolaji, O.S., Doumbia, V., 2017. On the historical origins of the CEJ, DP2, and Ddyn current systems and their roles in the predictions of ionospheric responses to geomagnetic storms at equatorial latitudes. *Journal of Geophysical Research (Space Physics)* 122, 7827–7833. doi:10.1002/2017JA024132.
- Bailey, R.L., Halbedl, T.S., Schattauer, I., Römer, A., Achleitner, G., Beggan, C.D., Wesztergom, V., Egli, R., Leonhardt, R., 2017. Modelling geomagnetically induced currents in midlatitude Central Europe using a thin-sheet approach. *Annales Geophysicae* 35, 751–761. doi:10.5194/angeo-35-751-2017.
- Baumjohann, W., Treumann, R.A., 1999. Basic Space Plasma Physics. Imperial College Press, 57 Shelton Street Covent Garden London WC2H 9HE.
- Blanc, M., Caudal, G., 1985. The spatial distribution of magnetospheric convection electric fields at ionospheric altitudes: a review. II. Theories. *Annales Geophysicae* 3, 27–42.
- Blanc, M., Richmond, A.D., 1980. The ionospheric disturbance dynamo. 1669–1686. doi:10.1029/JA085iA04p01669.
- Bobova, V.P., Vladimirkii, B.M., Pudovkin, M.I., 1985. The presence in the AE index of 160-minute pulsations evidently caused by solar pulsations. *Izvestiya Ordona Trudovogo Krasnogo Znameni Krymskogo Astrofizicheskogo Observatorii* 71, 19–25.
- Carrillo-Vargas, A., Pérez-Enríquez, R., Rodríguez-Martínez, M., López-Montes, R., Casillas-Pérez, G.A., Araujo-Pradere, E.A., 2012. Ionospheric disturbances detected by MEXART. *Advances in Space Research* 49, 1570–1580. doi:10.1016/j.asr.2011.12.017.
- Corona-Romero, P., Sanchez-Garcia, E., Sergeeva, M., Gonzalez-Esparza, J., Cifuentes-Nava, G., Hernandez-Quintero, E., Caccavari, A., Aguilar-Rodriguez, E., Mejía-Ambriz, J., de-la-Luz, V., Gonzalez, L., 2018. Kmex: the mexican geomagnetic k index, in: Proceedings of the II Pan-American Workshop on Geomagnetism, Basouras, Brazil, pp. 96–100.
- Corona-Romero, P., Sergeeva, M., Gonzalez-Esparza, J., Cifuentes-Nava, G., Hernandez-Quintero, E., Caccavari, A., Sanchez-Garcia, E., 2017. Mexican geomagnetic k index , 1–6.
- C.T Russell, J. G. Luhman, R.J.S., 2016. SPACE PHYSICS AN INTRODUCTION. Cambridge university press. University Princting House, Cambridge CB2 (BS, United Kingdom).
- da Silva Barbosa, C., Hartmann, G.A., Pinheiro, K.J., 2015. Numerical modeling of geomagnetically induced currents in a Brazilian transmission line. *Advances in Space Research* 55, 1168–1179. doi:10.1016/j.asr.2014.11.008.
- Denisenko, V.V., Zamai, S.S., Kitaev, A.V., Matveenkov, I.T., Pivovarov, V.G., 1992. System of ionospheric currents excited by a magnetospheric generator in the boundary layer. *Geomagnetism and Aeronomy* 32, 142–145.
- Gjerloev, J.W., 2012. The SuperMAG data processing technique. *Journal of Geophysical Research (Space Physics)* 117, A09213. doi:10.1029/2012JA017683.
- Gonzalez, W.D., Joselyn, J.A., Kamide, Y., Kroehl, H.W., Rostoker, G., Tsurutani, B.T., Vasiliunas, V.M., 1994. What is a geomagnetic storm? 5771–5792. doi:10.1029/93JA02867.
- Gonzalez-Esparza, A., Carrillo, A., Andrade, E., Jeyakumar, S., Ananthakrishnan, S., Praveenkumar, A., Sankarasubramanian, G., Suresh Kumar, S., Sierra, P., Vazquez, S., Perez-Enriquez, R., Kurtz, S., 2005. MEXART Measurements of Radio Sources. Interplanetary Scintillation Array in Mexico, in: AGU Fall Meeting Abstracts, pp. SH51C–1218.
- Gonzalez-Esparza, J.A., De la Luz, V., Corona-Romero, P., Mejía-Ambriz, J.C., Gonzalez, L.X., Sergeeva, M.A., Romero-Hernandez, E., Aguilar-Rodriguez, E., 2017. Mexican space weather service (sciesmex). *Space Weather* 15, 3–11. URL: <https://agupubs.onlinelibrary.wiley.com/doi/abs/10.1002/2016SW001496>, doi:<https://doi.org/10.1002/2016SW001496>.
- Hejda, P., Bochníček, J., 2005. Geomagnetically induced pipe-to-soil voltages in the Czech oil pipelines during October–November 2003. *Annales Geophysicae* 23, 3089–3093. doi:10.5194/angeo-23-3089-2005.
- Heppner, J.P., 1972a. Electric Fields in the Magnetosphere, in: Dyer, E.R. (Ed.), *Critical Problems of Magnetospheric Physics*, p. 107.
- Heppner, J.P., 1972b. Polar-cap electric field distributions related to the interplanetary magnetic field direction. 4877–4887. doi:10.1029/JA077i025p04877.
- Kikuchi, T., Hashimoto, K.K., 2016. Transmission of the electric fields to the low latitude ionosphere in the magnetosphere-ionosphere current circuit. *Geoscience Letters* 3, 4. doi:10.1186/s40562-016-0035-6.
- Knecht, D., B.M., S., 1985. *HANDBOOK OF GEOPHYSICS AND THE SPACE ENVIRONMENT*, chapter 4, THE GEOMAGNETIC FIELD. ed by A. S. Jursa, Boston: Air Force Geophysics Laboratory.
- Le Huy, M., Amory-Mazaudier, C., 2005. Magnetic signature of the ionospheric disturbance dynamo at equatorial latitudes: “ D_{dyn} ”. *Journal of Geophysical Research (Space Physics)* 110, A10301. doi:10.1029/2004JA010578.
- López-Montes, R., Pérez-Enríquez, R., Araujo-Pradere, E.A., 2012. The impact of large solar events on the total electron content of the ionosphere at mid latitudes. *Advances in Space Research* 49, 1167–1179. doi:10.1016/j.asr.2012.01.008.
- Martínez-Bretón L., J., Ortega, B.M., Hernandez-Quintero, J.E., 2016. Relationship between the minima of the horizontal magnetic component measured in mexico and the dst and sym-h indices for geomagnetic storms with $dst \leq 100$ nT during the descending phase of solar cycle 23. *Geofísica Internacional* 55, 155–164.
- Mayaud, P.N., 1980. Derivation, Meaning, and Use of Geomagnetic Indices. *Geophysical Monograph Series* 22, 607. doi:10.1029/GM022.
- Merline Matamba, T., Habarulema, J.B., Burešová, D., 2016. Midlatitude ionospheric changes to four great geomagnetic storms of solar cycle 23 in Southern and Northern Hemispheres. *Space Weather* 14, 1155–1171. doi:10.1002/2016SW001516.

- Nishida, A., 1966. Formation of plasmapause, or magnetospheric plasma knee, by the combined action of magnetospheric convection and plasma escape from the tail. 5669–5679. doi:[10.1029/JZ071i023p05669](https://doi.org/10.1029/JZ071i023p05669).
- Nishida, A., 1968a. Coherence of geomagnetic DP 2 fluctuations with interplanetary magnetic variations. 5549–5559. doi:[10.1029/JA073i017p05549](https://doi.org/10.1029/JA073i017p05549).
- Nishida, A., 1968b. Geomagnetic D_p 2 fluctuations and associated magnetospheric phenomena. 1795–1803. doi:[10.1029/JA073i005p01795](https://doi.org/10.1029/JA073i005p01795).
- Obayashi, T., Nishida, A., 1968. Large-Scale Electric Field in the Magnetosphere. doi:[10.1007/BF00362569](https://doi.org/10.1007/BF00362569).
- Pérez-Enríquez, R., Kotsarenko, A., 2003. IPS data of the Mexican Array Radio Telescope (MEXART) corrected for ionospheric scintillation and geomagnetic activity, in: EGS - AGU - EUG Joint Assembly, p. 2923.
- Pirjola, R., 2000. Geomagnetically induced currents during magnetic storms. IEEE Transactions on Plasma Science 28, 1867–1873. doi:[10.1109/27.902215](https://doi.org/10.1109/27.902215).
- Rishbeth, H., Garriott, O.K., 1969. Introduction to ionospheric physics.
- Rodriguez-Martinez, M., Perez-Enriquez, R., Carrillo-Vargas, A., Lopez-Montes, R., Araujo-Pradere, E.A., Casillas-Perez, G., Lopez Cruz-Abeyro, J., 2011. Ionospheric Disturbance Effects on IPS signals from MEXART, in: AGU Fall Meeting Abstracts, pp. SH13B–1969.
- Rodriguez-Martinez, M., Perez-Enriquez, R., Carrillo-Vargas, A., Lopez-Montes, R., Araujo-Pradere, E., Casillas, G., Lopez Cruz-Abeyro, J., 2011. Ionospheric disturbance effects on ips signals from mexart. AGU Fall Meeting Abstracts , 1969–.
- Rodriguez-Martinez, M., Pérez-Enríquez, H., Carrillo-Vargas, A., López-Montes, R., Araujo-Pradere, E., Casillas, G., Lopez Cruz-Abeyro, J., 2014. Ionospheric disturbances and their impact on ips using mexart observations. Solar Physics 289. doi:[10.1007/s11207-014-0496-8](https://doi.org/10.1007/s11207-014-0496-8).
- Romero-Hernandez, E., Gonzalez-Esparza, J.A., Rodriguez-Martinez, M., Sergeeva, M.A., Aguilar-Rodriguez, E., Mejia-Ambriz, J.C., De la Luz, V., 2017. Study of ionospheric disturbances over Mexico associated with transient space weather events. Advances in Space Research 60, 1838–1849. doi:[10.1016/j.asr.2017.06.042](https://doi.org/10.1016/j.asr.2017.06.042).
- Schrijver, C.J., 2015. Socio-Economic Hazards and Impacts of Space Weather: The Important Range Between Mild and Extreme. Space Weather 13, 524–528. doi:[10.1002/2015SW001252](https://doi.org/10.1002/2015SW001252), arXiv:1507.08730.
- Sergeeva, M.A., Gonzalez-Esparza, J.A., Blagoveshchensky, D.V., Maltseva, O.A., Chernov, A.G., Corona-Romero, P., De la Luz, V., Mejia-Ambriz, J.C., Gonzalez, L.X., Romero-Hernandez, E., Rodriguez-Martinez, M., Aguilar-Rodriguez, E., Andrade, E., Villanueva, P., Gatica-Acevedo, V.J., 2019. First observations of oblique ionospheric sounding chirp signal in Mexico. Results in Physics 12, 1002–1003. doi:[10.1016/j.rinp.2018.12.077](https://doi.org/10.1016/j.rinp.2018.12.077).
- Sergeeva, M.A., Maltseva, O.A., Gonzalez-Esparza, J.A., De la Luz, V., Corona-Romero, P., 2017. Features of TEC behaviour over the low-latitude North-American region during the period of medium solar activity. Advances in Space Research 60, 1594–1605. doi:[10.1016/j.asr.2017.06.021](https://doi.org/10.1016/j.asr.2017.06.021).
- van de Kamp, M., 2013. Harmonic quiet-day curves as magnetometer baselines for ionospheric current analyses. Geoscientific Instrumentation, Methods and Data Systems 2, 289–304. doi:[10.5194/gi-2-289-2013](https://doi.org/10.5194/gi-2-289-2013).
- Vodyannikov, V.V., Gordienko, G.I., Nechaev, S.A., Sokolova, O.I., Khomutov, S.Y., Yakovets, A.F., 2006. Geomagnetically induced currents in power lines according to data on geomagnetic variations. Geomagnetism and Aeronomy 46, 809–813. doi:[10.1134/S0016793206060168](https://doi.org/10.1134/S0016793206060168).
- Wei, Y., Zhao, B., Li, G., Wan, W., 2015. Electric field penetration into Earth's ionosphere: a brief review for 2000–2013. Science Bulletin 60, 748–761. doi:[10.1007/s11434-015-0749-4](https://doi.org/10.1007/s11434-015-0749-4).
- Younas, W., Amory-Mazaudier, C., Khan, M., Fleury, R., 2020. Ionospheric and Magnetic Signatures of a Space Weather Event on 25–29 August 2018: CME and HSSWs. Journal of Geophysical Research (Space Physics) 125, e27981. doi:[10.1029/2020JA027981](https://doi.org/10.1029/2020JA027981).
- Zaka, K.Z., Kobeia, A.T., Assamoi, P., Obrou, O.K., Doumbia, V., Boka, K., Adohi, B.J.P., Mene, N.M., 2009. Latitudinal profile of the ionospheric disturbance dynamo magnetic signature: comparison with the DP2 magnetic disturbance. Annales Geophysicae 27, 3523–3536. doi:[10.5194/angeo-27-3523-2009](https://doi.org/10.5194/angeo-27-3523-2009).

5. Appendix

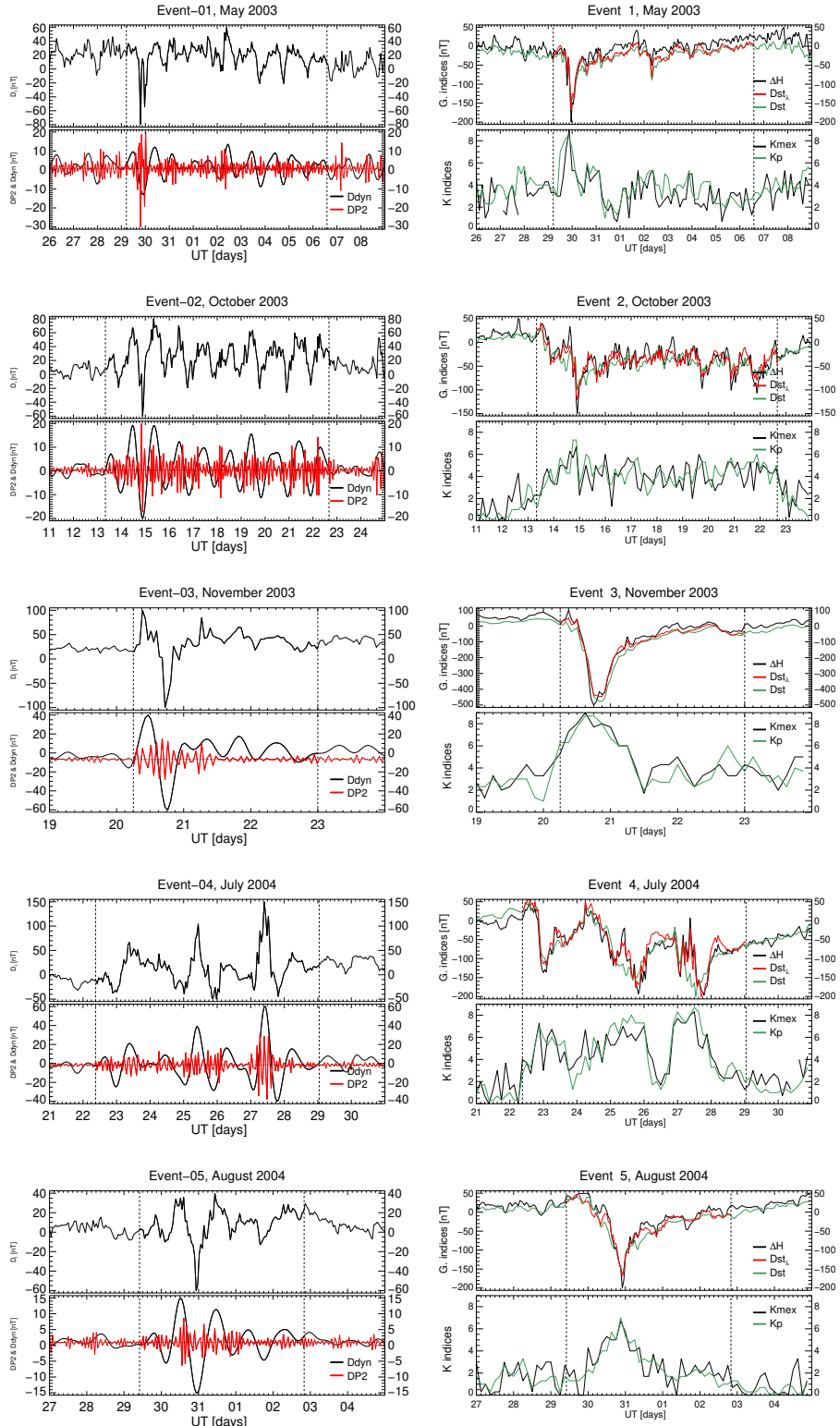


Figure 6: On the right side, top panels illustrate the contribution of Ionospheric Magnetic Disturbances, while bottom panels depict the isolated geomagnetic contributions of Ddyn and DP2. The vertical dashed lines highlight the geomagnetic storm time period during which such calculations are valid. On the left side, green lines represent planetary indices, while black lines denote local indices. Additionally, red lines represent the approximation of ΔH at top, while bottom showcases the comparison of local K (black line) and planetary k (green line).

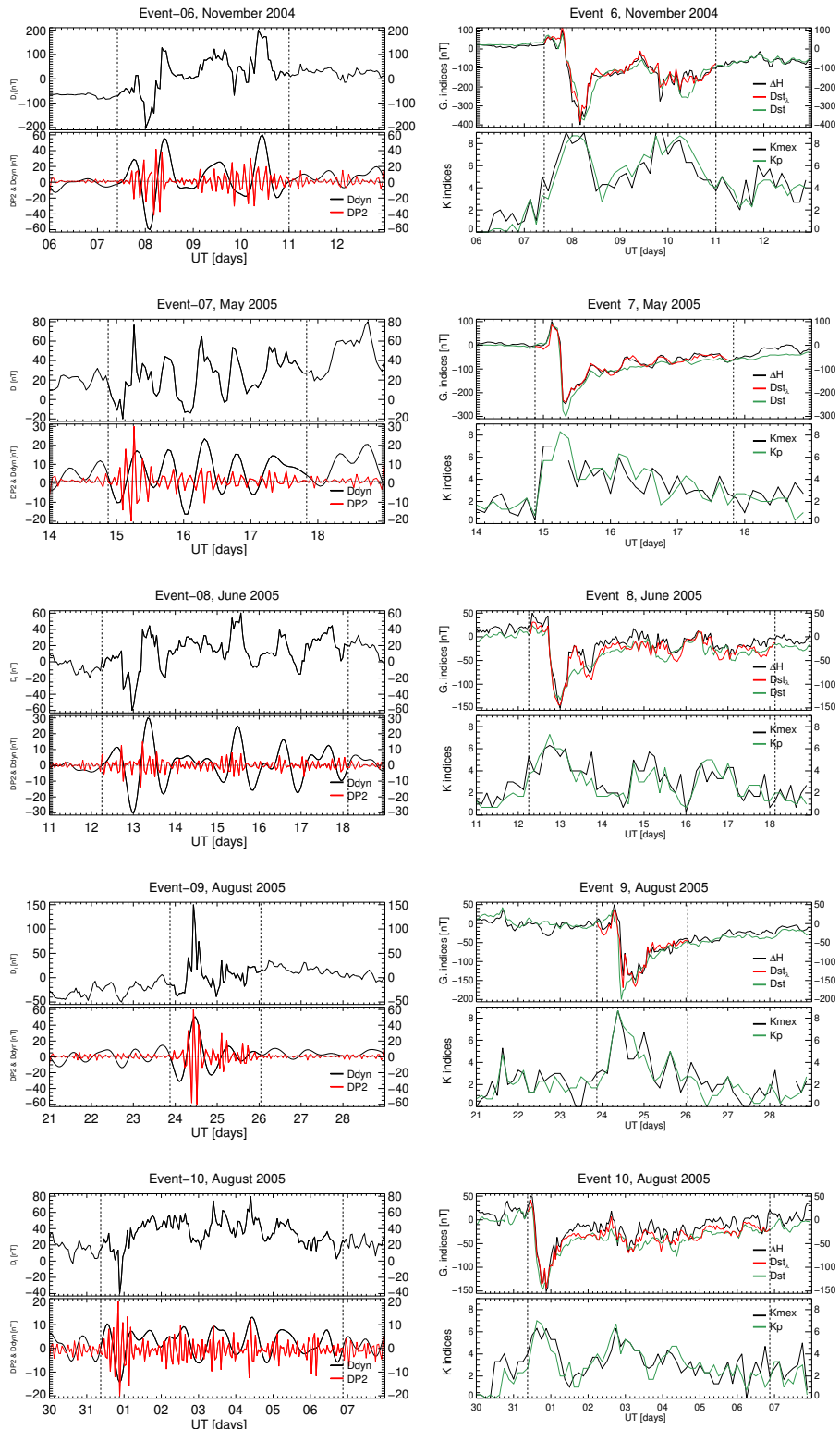


Figure 7: On the right side, top panels illustrate the contribution of Ionospheric Magnetic Disturbances, while bottom panels depict the isolated geomagnetic contributions of D_{dyn} and DP_2 . The vertical dashed lines highlight the geomagnetic storm time period during which such calculations are valid. On the left side, green lines represent planetary indices, while black lines denote local indices. Additionally, red lines represent the approximation of ΔH at top, while bottom showcases the comparison of local K (black line) and planetary k (green line).

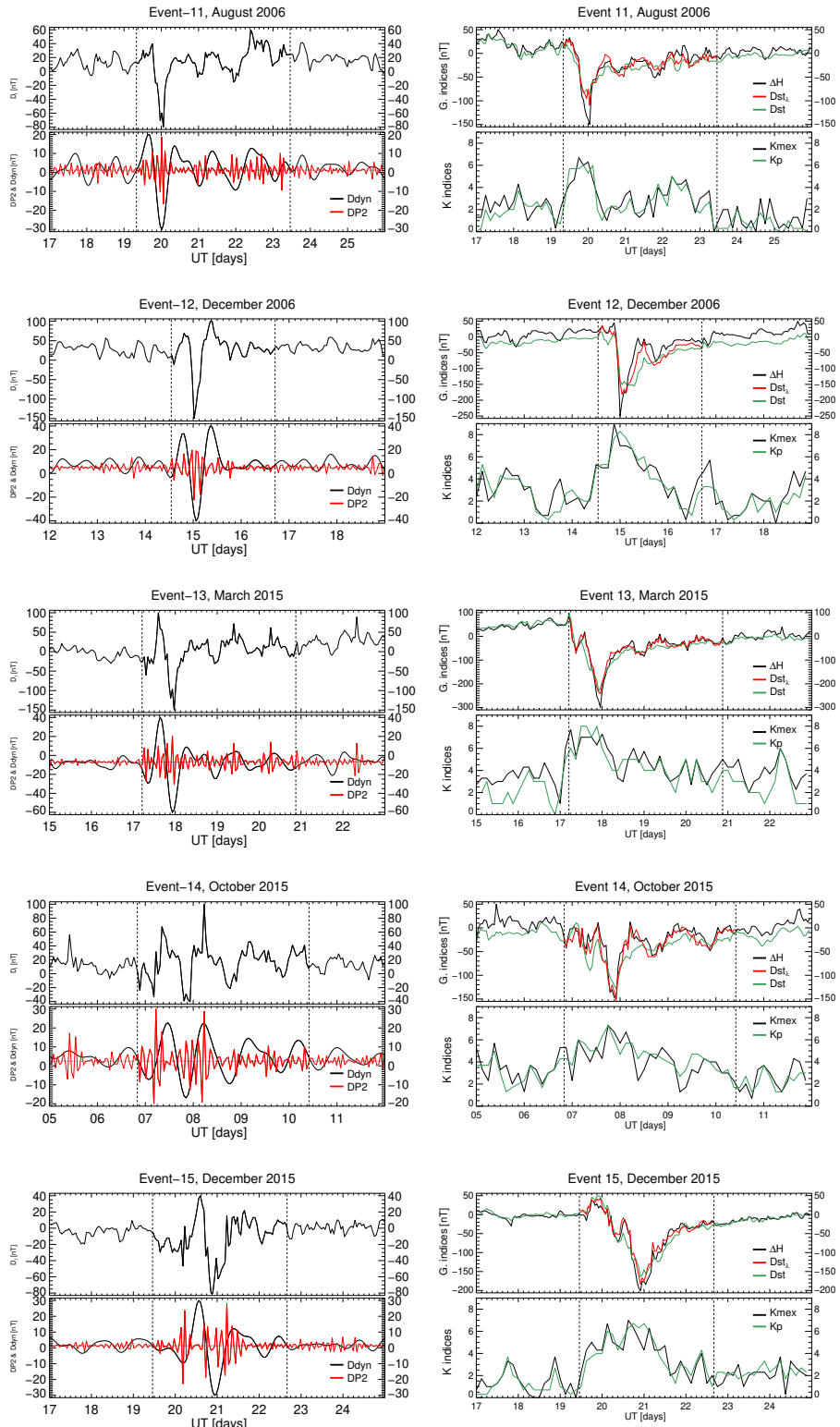


Figure 8: On the right side, top panels illustrate the contribution of Ionospheric Magnetic Disturbances, while bottom panels depict the isolated geomagnetic contributions of Ddyn and DP2. The vertical dashed lines highlight the geomagnetic storm time period during which such calculations are valid. On the left side, green lines represent planetary indices, while black lines denote local indices. Additionally, red lines represent the approximation of ΔH at top, while bottom showcases the comparison of local K (black line) and planetary k (green line).

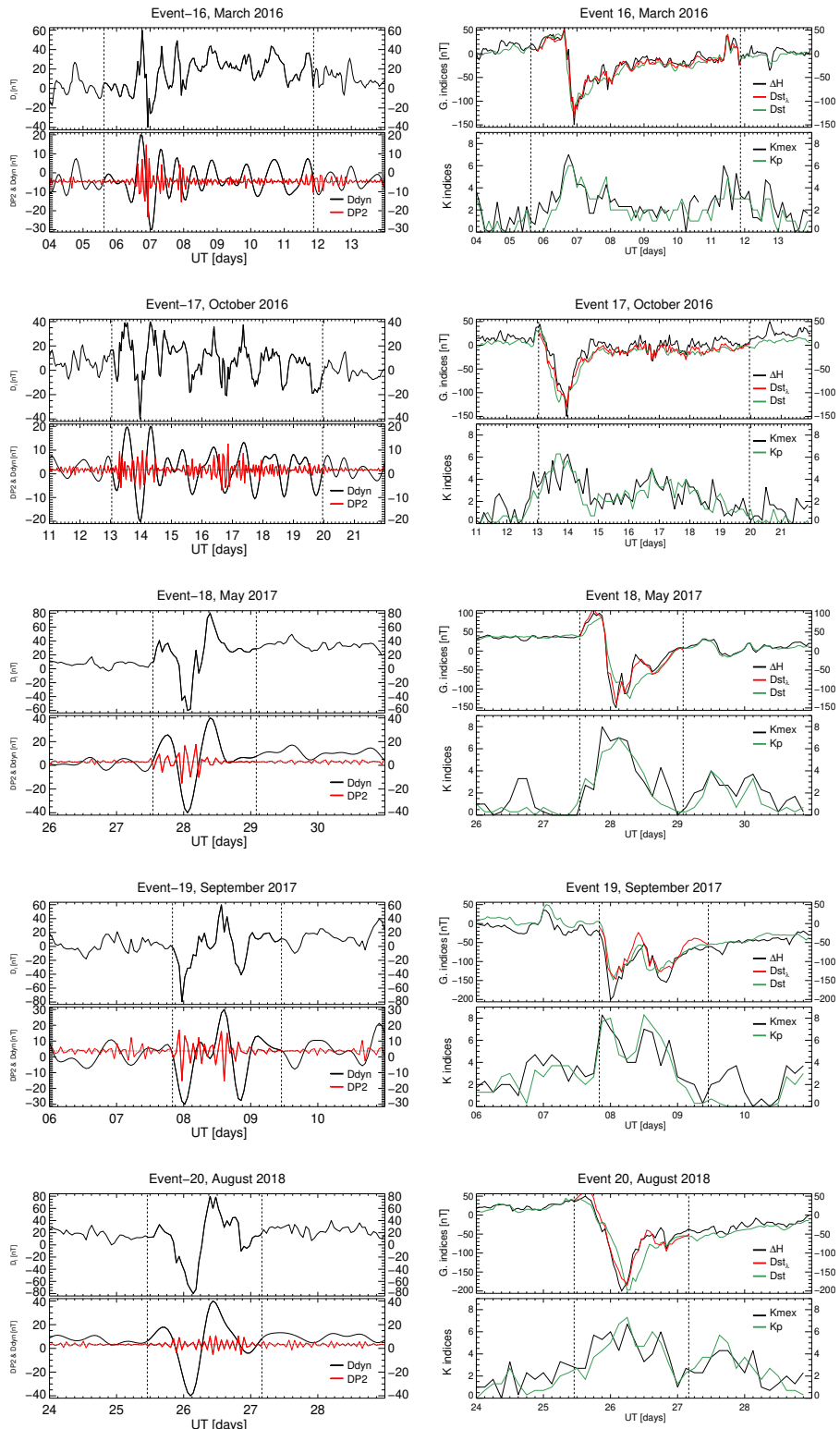


Figure 9: On the right side, top panels illustrate the contribution of Ionospheric Magnetic Disturbances, while bottom panels depict the isolated geomagnetic contributions of D_{dyn} and DP_2 . The vertical dashed lines highlight the geomagnetic storm time period during which such calculations are valid. On the left side, green lines represent planetary indices, while black lines denote local indices. Additionally, red lines represent the approximation of ΔH at top, while bottom showcases the comparison of local K (black line) and planetary k (green line).